Incorporating the LEMP Impact on Lightning Surge Analysis of Transmission Lines in EMT Simulators

Akifumi Yamanaka, *Member, IEEE*, Kazuyuki Ishimoto, *Member, IEEE*, and Akiyoshi Tatematsu, *Senior Member, IEEE*

***Abstract*—Electromagnetic transient (EMT) analysis is an important tool to estimate the lightning performance of transmission lines. In this paper, we advanced the EMT analysis method for transmission lines by incorporating the lightning electromagnetic pulse (LEMP) impact. Analyses by the proposed method clarify the mechanism of the LEMP impact on lightning overvoltages of transmission lines: the LEMP induces voltages having a polarity opposite to those generated by the lightning current, and these LEMP-induced voltages increase the insulator voltages; the EMT analysis without considering the LEMP impact provides lower insulator voltages for both struck and nearby towers. The models used in the proposed method can be synthesized immediately and straightforwardly from the geometries of the towers and lines, and the analysis can be performed within a short time. Moreover, various transmission lines—500, 275, and 77 kV class vertical double-circuit lines and a 275 kV class horizontal single-circuit line—were studied assuming a ground resistivity ranging from 0 to 5000 Ωm, and all the results were validated by the three-dimensional finite-difference time-domain method for solving Maxwell's equations. Thus, the proposed method is a powerful tool and has a potential impact on the lightning performance assessment of transmission lines and insulation coordination studies.**

***Index Terms*—EMT analysis, FDTD method, field-to-line coupling formula, LEMP, lightning, transmission lines.**

I. Introduction

LIGHTNING strikes to transmission lines cause disturbances to the operation of electric power systems. The main concern for the lightning protection of transmission lines is direct lightning events, causing back-flashovers or shielding failure flashovers. These phenomena have long been intensively studied and some standardized procedures for the estimation of the lightning performance of transmission lines as well as protection measures have been developed and utilized [1], [2], [3], [4].

Electromagnetic transient (EMT) analysis has been used for estimating the lightning performance of transmission lines. Modeling of transmission towers is one of the most important steps of EMT analysis since the towers are perpendicular to the ground and have sophisticated three-dimensional (3D) structures: the transverse electromagnetic (TEM) mode assumption, which can be applied to transmission lines, cannot be applied to such towers. Consequently, various models for transmission towers have been proposed by many researchers. One of the most frequently used models is the (cascade-connected) uniform distributed-parameter line representation of towers using surge impedance values calculated by appropriate formulae for the studied tower shape and/or lightning phenomena [5], [6], [7], [8], [9]. The multistory tower model [10] is also frequently used owing to its simplicity and flexibility to tune the calculated insulator voltages [11], [12], [13], [14]. There are other EMT analysis models of transmission towers, and ref. [15] provides a quite informative review.

Progress in numerical electromagnetic analysis (NEA) techniques has enabled a more accurate analysis of a lightning strike to transmission towers than EMT analysis [16], [17], [18], [19], [20], [21], [22]. This is because NEA can directly model tower structures, a lightning channel including the electromagnetic pulse (LEMP) radiation and coupling, grounding structures, and others. The accuracy of NEA for lightning surge studies has been validated by reproducing various experimental and observational results. The difference between the insulator voltages calculated by NEA and conventional EMT analysis has been pointed out [23], [24], [25], [26].

Although NEA is advantageous from the viewpoint of accuracy compared with EMT analysis, EMT analysis is still and will be preferred and utilized for the estimation of the lightning performance of transmission lines because of its simplicity and much shorter calculation time than NEA: the estimation of lightning performance requires a large number of analyses considering various conditions [27], [28], [29], [30], [31]. The conditions include, for instance, lightning current parameters and waveforms, electrical parameters of soil, power frequency voltages, and design parameters of transmission lines—the number of overhead grounding wires (OHGWs) and their geometry, insulation level, the installation of additional lightning protection equipment such as surge arresters, and tower grounding resistance.

In this view, to achieve both high accuracy and short computation time, improvements of EMT analysis models based on NEA results have been proposed recently. Examples include the modeling of the tower and line considering non-TEM characteristics [24], [32], modifications of the parameters of the multistory tower model [25], and the black-box modeling [33].

Manuscript received 25 September 2023; revised 23 January 2024; accepted 24 March 2024. Date of publication 27 March 2024; date of current version 23 May 2024. Paper no. TPWRD-01340-2023. *(Corresponding author: Akifumi Yamanaka.)*

The authors are with the Grid Innovation Research Laboratory, Central Research Institute of Electric Power Industry, Yokosuka-shi 240-0196, Japan (e-mail: yamanaka3929@criepi.denken.or.jp; ishimoto@criepi.denken.or.jp; akiyoshi@criepi.denken.or.jp).

Color versions of one or more figures in this article are available at https://doi.org/10.1109/TPWRD.2024.3382316.

Digital Object Identifier 10.1109/TPWRD.2024.3382316

These improvements are quite practical since accurate analysis can be performed in a short calculation time once the model is developed on the basis of the NEA results. However, the requirement of pre-NEA can be a drawback at the same time since it requires complicated modeling, large computational resources, and a longer calculation time. In addition, the impact of the lightning channel on insulator voltages [34], [35], [36] was not considered explicitly in EMT analysis.

In this paper, we propose an EMT analysis method that explicitly incorporates the LEMP impact on transmission lines. The proposed method is based on the method presented in [37], inspired by the analysis of medium voltage (MV) distribution lines revealing the LEMP impact on lightning overvoltages [38], [39], [40], [41]. The proposed method uses the uniform distributed-parameter line representation for transmission towers and hence does not need pre-NEA, which is required for the recently developed accurate EMT analysis models of transmission towers. Note that a method similar to the proposed method was presented in [34], [35]. However, using the proposed method, this paper clarifies the mechanism of the LEMP impact on lightning overvoltages of transmission lines. Moreover, the applicability of the method to various types of lines (500, 275, and 77 kV vertical double-circuit lines and a 275 kV horizontal single-circuit line) with a wide range of soil resistivities (from 0 to 5000 Ωm) are shown. The presented analyses are all validated by results derived using the 3D finite-difference time-domain (FDTD) analysis for solving Maxwell's equations [17]. Thus, the proposed method is practical and accurate for evaluating the lightning performance of transmission lines.

The following is the structure of this paper. In Section II, the proposed EMT analysis method considering the LEMP effect and the 3D FDTD method for solving Maxwell's equations are overviewed. In Section III, the specifications of the studied transmission lines are presented firstly, and then the details of the modeling techniques are described. Section IV shows the analysis results and discusses the mechanism generating insulator voltages and the features of the proposed method. In Section V, we conclude this paper.

II. Overview of the Analysis Method

A. EMT Analysis Considering the LEMP Effect

The proposed method is based on EMT analysis and includes three additional parts as shown in Fig. 1: (a) calculation of the current along the lightning channel, (b) calculation of the LEMP, and (c) solution of the Agrawal et al. formula [42] interfaced with EMT analysis [37]. These additional parts are overviewed in this section.

1) Part (a). Calculation of the Current Along the Channel: To calculate the LEMP from the lightning channel, the current along the channel should be calculated. Since the lightning channel is represented by a current source in parallel with a constant resistance representing the lightning channel impedance in EMT analysis, the channel base current can be simply derived by the sum of the output of the current source and the current through the lightning channel impedance model. Then, the current along the lightning channel can be calculated from the channel base current by properly considering the traveling time delay and attenuation. In this paper, the lightning channel was modeled using the transmission line model with a constant current traveling speed without attenuation.

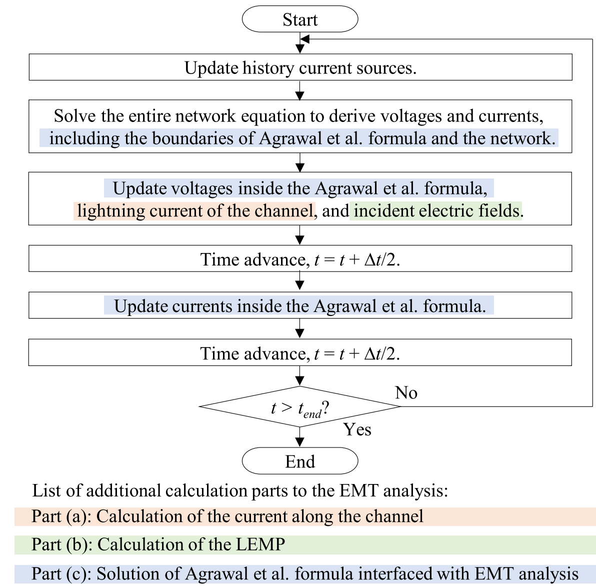

Fig. 1. Flowchart for the EMT analysis considering the LEMP impact.

Note that although the method presented in [37] can include the struck object for the LEMP calculation, it was not considered in this paper. This comes from the implication from the previous study, i.e., in the case in which the LEMPs from only the lightning channel are considered, a simplified model for the struck object provides accurate analysis results [37]; a simpler modeling is better from a practical viewpoint. Details of EMT analysis models are presented in Section III-C. The effect of the first descending current wave and its multiple reflections along a tall object on the LEMP is significant, as studied with simultaneous observations of a lightning current at the object and remote fields (e.g., [43], [44], [45], [46], [47]). However, this effect may not be significant for most of negative first strokes to transmission towers to discuss insulator voltages since the front duration of the current is sufficiently longer than the round-trip time of the traveling wave along the tower. The presence of OHGWs may also weaken the effect. As shown in Section IV-A, the proposed method can provide accurate insulator voltages. Nevertheless, the response to fast front currents is important and this aspect will be discussed in Section IV-D.

2) Part (b). Calculation of the LEMP: Using the channel base current, we derive the LEMP—electric fields required for the Agrawal et al. formula for induced voltage calculation—by the potential method [48]. On the basis of the assumption presented in [37], [48], a scalar potential at (x, y, z) generated by a unit step charge traveling from a channel base point (x_l, y_l, z_l), as shown in Fig. 2, can be calculated as

$$\phi = \frac{1}{4\pi\varepsilon_0 v} \ln \frac{vt - \xi_1 + \sqrt{(vt - \xi_1)^2 + (1 - \beta^2)(r_1^2 - \xi_1^2)}}{(1 + \beta)(r_1 - \xi_1)}, \tag{1}$$

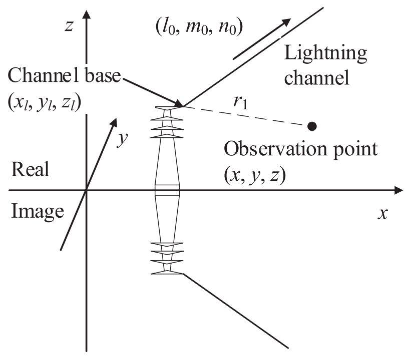

Fig. 2. Lightning channel and its image for computing scalar and vector potentials at observation point (x, y, z).

where t is time, ε_0 is the permittivity in free space, and β is the ratio of the current traveling speed along the channel v to the speed of light in free space, c_0. The variables r_1 and ξ_1 are

$$r_1 = \sqrt{(x - x_l)^2 + (y - y_l)^2 + (z - z_l)^2}, \quad (2)$$

$$\xi_1 = l_0 (x - x_l) + m_0 (y - y_l) + n_0 (z - z_l), \quad (3)$$

where l_0, m_0, and n_0 are the direction cosines of the channel. Although the potential method can model an inclined channel by setting l_0, m_0, and n_0 to appropriate values and even a bent or tortuous channel by superimposition [48], in this paper, we focus on the straight and vertical channels. The image charge generates the following scalar potential:

$$\phi' = \frac{-1}{4\pi\varepsilon_0 v} \ln \frac{vt - \xi_2 + \sqrt{(vt - \xi_2)^2 + (1 - \beta^2)(r_2^2 - \xi_2^2)}}{(1 + \beta)(r_2 - \xi_2)}, \quad (4)$$

where

$$r_2 = \sqrt{(x - x_l)^2 + (y - y_l)^2 + (z + z_l)^2}, \quad (5)$$

$$\xi_2 = l_0 (x - x_l) + m_0 (y - y_l) - n_0 (z + z_l). \quad (6)$$

The total scalar potential ϕ_s is given by the sum of the real and image potentials with an appropriate time delay:

$$\phi_s = \phi u (t - r_1/c_0) + \phi' u (t - r_2/c_0), \quad (7)$$

where $u(t)$ is Heaviside's step function. In the same manner, the vector potential $\boldsymbol{A_v}$ can be calculated, and finally, the electric field radiated from the lightning channel is calculated as

$$\boldsymbol{E} = -\nabla\phi_s - \frac{\partial \boldsymbol{A_v}}{\partial t}. \quad (8)$$

Since this field is the step response, the field generated by an arbitrary current waveform is calculated using the convolution integral.

3) Part (c). Solution of Agrawal et al. Formula Interfaced With EMT Analysis: To consider the induced voltages by the LEMP in EMT analysis, the electric field is transferred to the part for solving the Agrawal et al. formula [42]:

$$\frac{\partial v^s(x,t)}{\partial x} + L' \frac{\partial i(x,t)}{\partial t} + \int_0^t \xi_g (t - \tau) \frac{\partial i(x,t)}{\partial t} \mathrm{d}\tau = E_x^i (x, h, t), \quad (9)$$

$$\frac{\partial i(x,t)}{\partial x} + C' \frac{\partial v^s(x,t)}{\partial t} = 0, \quad (10)$$

where v^s and i are the scattered voltage and total current; x and h are the line position and heigh; L' and C' are the inductance and capacitance of the line; $E_x{}^i$ and ξ_g are the incident horizontal electric field and ground impedance, respectively. The total voltage v^t is calculated by considering the incident voltage v^i derived from the incident vertical electric field $E_z{}^i$ as follows:

$$v^t(x,t) = v^s(x,t) + v^i(x,t) = v^s(x,t) - \int_0^h E_z^i (x, z, t) \, \mathrm{d}z. \quad (11)$$

In the presented method, the Agrawal et al. formula is solved by the point-centered FDTD method. Update equations for the discretized scattered voltage $v_k{}^n$ and current $i_{k+1/2}^{n+1/2}$ (k and n are the indexes for spatial and temporal discretization with length Δx and time Δt) are [37]

$$v_k^n = v_k^{n-1} - \frac{\Delta t}{\Delta x} C'^{-1} \left(i_{k+1/2}^{n-1/2} - i_{k-1/2}^{n-1/2} \right), \quad (12)$$

$$i_{k+1/2}^{n+1/2} = -K_1 K_2 i_{k+1/2}^{n-1/2} - K_1 \left(x'^{n+1/2}_{k+1/2} + x'^{n-1/2}_{k+1/2} \right) - \frac{1}{\Delta x} K_1 \left(v_k^n - v_{k-1}^n \right) + K_1 E_{k+1/2}^n, \quad (13)$$

where H_0 and x' are terms for considering the ground impedance, $E_{k+1/2}^n$ is the incident horizontal electric field, and coefficients K_1 and K_2 are

$$K_1 = \left(H_0/2 + L'/\Delta t \right)^{-1}, K_2 = H_0/2 - L'/\Delta t. \quad (14)$$

The boundaries of each Agrawal et al. formula should be connected to nodes of the network equation of the EMT analysis (in this paper the Agrawal et al. formula is connected to transmission tower models). The Agrawal et al. formula and the EMT analysis are interfaced considering the presence of distributed capacitance at both ends of the formula. For instance, the leftmost node of the Agrawal et al. formula and the node of the EMT analysis are interfaced with the history current source and equivalent conductance as follows [37]:

$$i_{c0}^n = G_c v_{c0}^n + J_{c0}^n, \quad (15)$$

$$G_c = \frac{C' \Delta x}{2\Delta t}, J_{c0}^n = -G_c v_{c0}^{n-1} + 2 \left(i_{1/2}^{n-1/2} - \frac{i_{c0}^{n-1}}{2} \right), \quad (16)$$

where $i^n{}_{c0}$ is the current of the EMT analysis, and $v^n{}_{c0}$ is the voltage of the leftmost node of the Agrawal et al. formula and at the same time the node voltage of the EMT analysis.

As shown in (9)–(11), the Agrawal et al. formula can be described as telegrapher's equations considering the external excitation. Therefore, using this formula interfaced with EMT analysis by (15), both the induced voltages by the LEMP and the

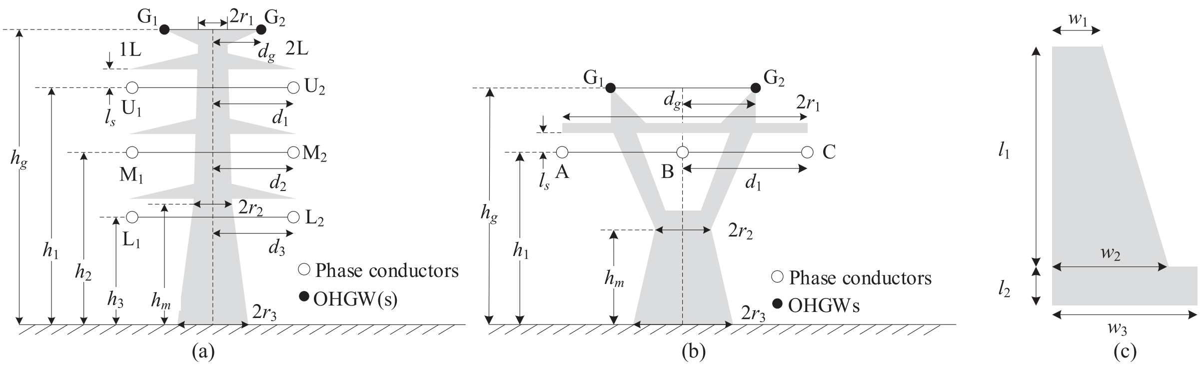

Fig. 3. Definition of the geometry of the studied towers. (a) Vertical double-circuit tower, (b) horizontal single-circuit tower, and (c) tower foundation.

voltages generated by the lightning current (direct-stroke effect) can be calculated at the same time.

B. 3D FDTD Method for Solving Maxwell's Equations

The FDTD method directly solves Maxwell's equations in the time domain using differences for spatial and temporal derivatives. This method is more suitable for analyzing lightning surges of transmission lines than EMT analysis since lightning surges include dynamic electromagnetic phenomena, such as the LEMPs radiated from a lightning channel, the coupling of the LEMPs and transmission lines, and current traveling along a 3D sophisticated structure of a transmission tower. Owing to the development of analysis techniques dedicated to lightning surge studies and computational resources, the FDTD method has become one of the most powerful NEA methods for analyzing lightning surges [16].

In this paper, the results of the FDTD analysis performed with the Virtual Surge Test Lab. Restructured and Extended Version (VSTL REV) [49] were used as a reference. Although any numerical method contains inaccuracies, various observational and experimental results were reproduced by VSTL REV [50], [51], [52], [53], [54]. The modeling approaches presented in Section III-B follow those adopted in literature including the cell size, and thus the FDTD analysis results can be considered as a reference.

III. Analysis Cases and Models

A. Specifications of the Studied Transmission Lines

The following four transmission lines were analyzed.

1) 500 kV vertical double-circuit line (500)
2) 275 kV vertical double-circuit line (275)
3) 77 kV vertical double-circuit line (77)
4) 275 kV horizontal single-circuit line (275-h)

Table I summarizes the conductor types of the lines and the geometries of the towers. The definition of the variables used in Table I(B) can be found in Fig. 3. The 77 kV line has a single OHGW, whereas the others have double OHGWs. Fig. 3(c) shows the tower foundation. In this paper, the use of additional grounding structures, such as counterpoise wires [55], [56], was not assumed: the four tower legs perform as a grounding structure of the tower.

TABLE I
Specifications of the Transmission Line: (a) Conductor Types and (b) Geometries Unit in Meter

Voltage class [kV]	500	275	77	275-h
Phase conductor	TACSR	TACSR	TACSR	ACSR
Cross section [mm^2]	410	410	610	610
Diameter [mm]	28.5	28.5	34.2	34.2
Conductor per phase	6	4	1	1
Bundle separation [m]	0.5	0.5	—	—
OHGW	IACSR	KTACSR	AC	KTACSR
Cross section [mm^2]	150	120	70	120
Diameter [mm]	20.0	17.5	12.0	17.5
Span length, L_S [m]	400	350	300	300

(a)

Voltage class [kV]	500	275	77	275-h
h_g	79.0	52	37.8	26.5
h_1	71.0	43.0	34.3	18.0
h_2	57.0	35.5	31.0	—
h_3	42.0	28.0	27.0	—
d_g	14.0	6.5	—	4.75
d_1	11.0	6.0	2.5	8.25
d_2	11.0	6.5	4.0	—
d_3	12.0	7.0	2.8	—
h_m	36.5	27.8	27.0	15.5
r_1	3.0	1.5	0.25	6.5
r_2	3.0	1.5	0.5	2.6
r_3	9.0	5.0	3.0	3.5
l_s	4.0	2.5	1.0	2.0
l_1	4.0	3.0	2.5	2.5
l_2	1.0	1.0	0.5	0.5
w_1	1.0	0.5	0.5	0.5
w_2	2.0	1.0	1.0	1.0
w_3	3.0	2.0	1.5	1.5

(b)

B. 3D FDTD Analysis Model

In each analysis, five transmission towers were considered. Fig. 4 shows the FDTD analysis model, and Table II summarizes the analysis conditions. The FDTD analysis space of 1500–2000 × 1000 × 1500 m was divided into non-uniform cells having sizes depending on the type of transmission line, and the lines were modeled along the x-axis of the analysis space. Tower#3, which is located at the center of the analysis space, was

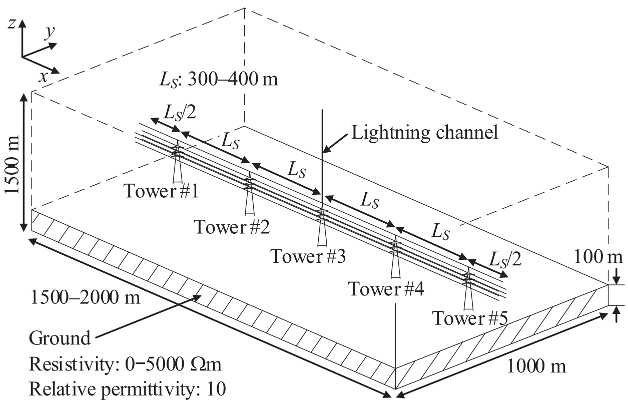

Fig. 4. FDTD analysis model (77 kV line is illustrated as an example).

TABLE II
FDTD ANALYSIS CONDITIONS

Voltage class [kV]	Analysis space $x \times y \times z$ [m]	Cell divisions $N_x \times N_y \times N_z$	Cell size [m]	Time step [ns]
500	2000×1000×1500	570×174×271	1.0–10	0.96
275	1750×1000×1500	600×190×346	0.5–10	0.48
77	1500×1000×1500	600×200×356	0.25–10	0.24
275-h	1500×1000×1500	760×232×317	0.25–10	0.24

considered a lightning-struck tower. Two nearby towers were modeled on both sides of the struck tower. Liao's second-order absorbing boundary condition [57], which is commonly used in 3D FDTD-based simulations (e.g., [16], [49], [50], [51], [52], [53], [54]), was adopted.

A straight and vertical lightning channel was modeled using the transmission line model with a current traveling speed of 100 m/μs. The transmission line model was represented by a phased-current-source array with a forced magnetic field [58], and thus the lightning channel impedance was set to infinity.

Although the finite channel impedance is considered in general, this paper adopted the current-source expression of the lightning channel to set the analysis condition of the FDTD method and EMT analysis identical, to perform a rigorous comparison. If the other electromagnetic model of lightning channel, such as an inductance-loaded thin wire with a voltage source, is employed [53], [59], it becomes difficult to inject the same lightning current, to consider the same channel impedance, and to consider the same temporal and spatial distribution of the current along the channel, between the FDTD method and the EMT analysis.

It is worth noting that the lightning channel impedance is generally much higher than the impedance of a transmission line tower struck by lightning [3] (nevertheless, the use of an appropriate channel impedance is preferable [60]). In addition, we have confirmed that the insulator voltages calculated using the channel model of the inductance-loaded thin wire with a voltage source by the FDTD method can be reproduced by the relevant modeling (with relevant return stroke speed and the finite channel impedance) by the proposed method.

The lightning channel was attached to the tip of the crossarm of the OHGW G_1 for the 500 kV tower and for both 275 kV vertical and horizontal towers, and to the top of the 77 kV tower.

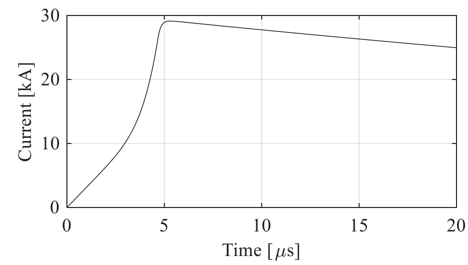

Fig. 5. Lightning current waveform synthesized by the CIGRE function.

The current waveform was synthesized by the CIGRE function [2], as shown in Fig. 5. The current peak, the equivalent wavefront derived from $t_{30/90}$/0.6, maximum steepness, and the tail time to half value were set to 29.3 kA, 3.2 μs, 18.9 kA/μs, and 70 μs, respectively. The wavefront parameters were adopted from the median parameters of the observed lightning currents on transmission towers in Japan [61].

The details of the modeling techniques are as follows. The tower structure was modeled using thin wires as detailed as possible. The inclined parts of the tower, such as tower legs and crossarms, were modeled by the staircase approximation. The model is similar to that used in [53]. The overhead lines including the phase conductors and OHGW(s) were modeled by a thin-wire representation method, which modifies the permittivity and permeability of the cells surrounding the conductor [62]. The lines were modeled as straight lines and the sag of the line [63] was not considered. The bundled phase conductors of 275 and 500 kV vertical double-circuit lines were modeled using a single conductor by setting their radii based on the geometric mean distance. Both ends of each overhead line were attached to the Liao's second-order boundary, which simulates a matched condition. The tower legs were modeled using rectangular perfect conductors following the dimensions shown in Fig. 3(c). The legs were buried under the ground having a thickness of 100 m. The resistivities of the ground were set to 0, 100, 500, 1000, and 5000 Ωm, and the relative permittivity was set to 10: the frequency-dependent (FD) characteristic of these parameters [64], [65] was not considered for simplicity, since the main interest of this study is to analyze the effect of voltages induced by the LEMP effect. The presence of an insulator string was not modeled explicitly. The insulator voltage was defined by the integral of the electric field between the tip of the tower crossarm and the phase conductor.

C. EMT Analysis Models

In this paper, the following three EMT analysis models were employed.

- EMT analysis considering the LEMP effect with simple tower model (Proposed)
- EMT analysis with simple tower model (Simple)
- EMT analysis with multistory tower model [10] (Multistory)

The simple tower model is a cascade of four uniform lines for the vertical double-circuit towers and a single uniform line for

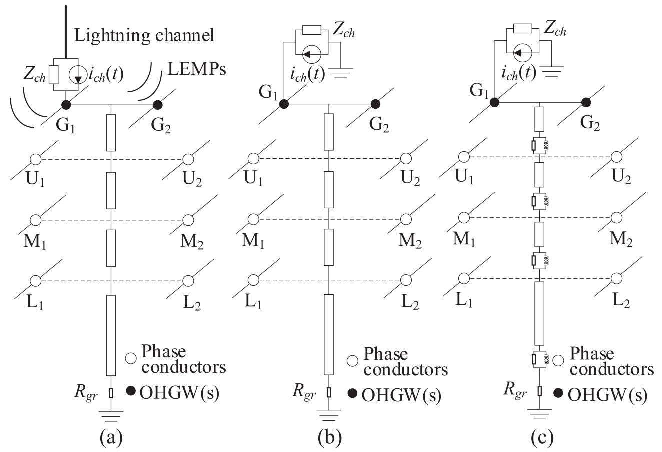

Fig. 6. EMT analysis models for vertical double-circuit tower with double OHGWs. (a) Proposed model: EMT analysis considering the LEMP effect with simple tower model (Proposed), (b) EMT analysis with simple tower model (Simple), (c) EMT analysis with multistory tower model (Multistory). The channel impedance Z_{ch} was set to infinity for rigorous comparison with the 3D FDTD analysis.

the horizontal single-circuit tower. The multistory tower model was employed for the vertical double-circuit towers and not for the horizontal single-circuit tower. The models for vertical double-circuit towers with double OHGWs are shown in Fig. 6.

This paper employed the simple tower model for the proposed method whereas various better tower models have been developed especially for vertical double-circuit towers. This is because these models are in general optimized to provide accurate insulator voltages with EMT analysis not explicitly considering the induced voltages by the LEMP from a return-stroke current. The present study focuses on the LEMP impact on lightning overvoltages, and thus the characteristics of the better tower models optimized for EMT analysis without LEMP should be disregarded in the first place. The comparison between "Proposed" and "Simple" models will clarify the LEMP impact. The "Multistory" model was employed here as a benchmark since it is one of the most widely used tower models. Indeed, the modeling of the tower characteristic is important and will be discussed in Section IV-A.

1) Tower Model: The surge impedance Z_t of the simple tower model for representing the vertical double-circuit towers was calculated using Modified Jordan's formula [9]:

$$Z_t = 60\left[\ln\left(4h_g/r_{ave}\right) - 1\right], \tag{17}$$

where h_g is the height of the tower, and r_{ave} is the equivalent radius of the tower calculated as

$$r_{ave} = \left\{r_1\left(h_g - h_m\right) + r_2 h_g + r_3 h_m\right\}/h_g. \tag{18}$$

The definition of each parameter can be found in Fig. 3.

The surge impedance of the horizontal single-circuit tower was calculated using Chisholm et al. formula [7]:

$$Z_t = 60\left\{\ln\left[\cot\left(\theta/2\right)\right]\right\}, \tag{19}$$

where the angle θ is calculated as

$$\theta = \arctan\left(r_{ave}/h_g\right). \tag{20}$$

TABLE III
SURGE IMPEDANCE OF THE STUDIED TRANSMISSION TOWERS

Voltage class [kV]	500	275	77	275-h
Z_t [Ω]	183	192	208	118

The equivalent radius r_{ave} was also calculated using (18). The calculated surge impedances are summarized in Table III.

For the multistory tower model, although many types of modification have been presented [11], [12], [13], the original parameters were adopted here as a reference: the surge impedances of the three upper parts and lower part of the tower were set to 220 and 150 Ω, respectively, and RL parameters were calculated as described in [10].

Note that the LEMP effect along the tower was not considered in this paper. Although the effect surely has an impact on the insulator voltages, the proposed method can provide sufficiently accurate insulator voltages as shown in Section IV. Nevertheless, the inclusion of the LEMP effect along the tower is an interesting and challenging topic to study.

2) Tower Footing Model: Pursuing simplicity, the tower grounding was modeled using a constant resistance R_{gr}, and the FD characteristics were not considered. Note that the FD characteristic of the tower grounding is inherently considered in the FDTD method [66], [67], and this characteristic may cause the difference in analysis results for high-soil-resistivity cases, as shown in Section IV-C.

The grounding resistance of a single tower leg R_{f1} is calculated as follows [4], [68]:

$$R_{f1} = 0.65\frac{\rho}{2\pi l_f}\left[\ln\left(\frac{4l_f}{r_f}\right) - 1\right], \tag{21}$$

where ρ is the soil resistivity, l_f is the length of the buried part of tower legs equal to l_1+l_2 (see Fig. 3(c)), and r_f is the equivalent radius of the leg. The radius r_f is calculated so that the surface of the equivalent cylinder having the radius r_f and length l_f becomes the same as that of the tower leg. The total grounding resistance of four legs R_{gr} is calculated as follows considering the mutual characteristic:

$$R_{gr} = \frac{R_{f1}}{4}\left[1 + \frac{l_f}{D_f}\frac{1+2\sqrt{2}}{\ln\left(4l_f/r_f\right) - 1}\right], \tag{22}$$

where D_f ($= 2\sqrt{2}r_3$) is the diagonal of the legs. The calculated resistance is presented in the leftmost columns of Tables IV–VII
.

3) Overhead Line Model: The overhead lines, including phase conductors and OHGW(s), were modeled using the Agrawal et al. formula [42]. As mentioned in Section II-A3, the Agrawal et al. formula interfaced with the EMT analysis can consider both the induced voltages by the LEMP and the voltages generated by the lightning current (direct-stroke effect). In the proposed method, the LEMP effect was considered by the incident electric field calculated by the potential formulae. On the other hand, in EMT analysis not considering the LEMP, the electric field (external excitation) was ignored, and the direct-stroke effect was only considered. The Cooray–Rubinstein formula was

TABLE IV
INSULATOR VOLTAGE PEAKS OF THE STRUCK TOWER DERIVED BY THE FDTD METHOD AND THE DIFFERENCES OF THE VOLTAGES DERIVED BY THE FDTD METHOD AND EMT ANALYSIS MODELS FOR THE 500 KV TOWER

ρ [Ωm], R_{gr} [Ω]	Phase	FDTD [V/A]	Proposed %	Simple %	Multi-story, %
ρ = 0, R_{gr} = 0	U_1	24.3	2.67	−45.8	−30.6
	M_1	20.4	4.68	−40.5	−32.9
	L_1	15.5	8.01	−34.1	−38.6
ρ = 100, R_{gr} = 1.63	U_1	25.4	0.42	−46.8	−32.9
	M_1	21.9	1.03	−42.5	−36.5
	L_1	17.4	1.95	−37.9	−43.6
ρ = 500, R_{gr} = 8.15	U_1	27.4	0.43	−43.7	−32.1
	M_1	24.6	0.95	−38.3	−34.6
	L_1	20.6	1.49	−32.6	−39.5
ρ = 1000, R_{gr} = 16.3	U_1	29.3	1.57	−39.5	−29.7
	M_1	27.0	2.46	−32.7	−30.7
	L_1	23.5	3.32	−25.5	−32.9
ρ = 5000, R_{gr} = 81.5	U_1	37.9	9.38	−17.3	−13.3
	M_1	38.3	12.0	−5.83	−7.30
	L_1	38.2	11.1	2.26	−3.57

TABLE VII
SAME AS TABLE IV, BUT FOR THE 275 KV SINGLE-CIRCUIT TOWER

ρ [Ωm], R_{gr} [Ω]	Phase	FDTD [V/A]	Proposed %	Simple %
ρ = 0, R_{gr} = 0	A	10.4	3.42	−55.6
	B	8.89	12.0	−50.4
	C	9.30	7.67	−50.1
ρ = 100, R_{gr} = 3.30	A	13.2	−2.11	−53.6
	B	11.6	3.57	−49.6
	C	12.1	−0.12	−49.9
ρ = 500, R_{gr} = 16.5	A	18.9	2.22	−34.7
	B	17.1	5.80	−31.2
	C	18.0	2.88	−31.1
ρ = 1000, R_{gr} = 33.0	A	24.0	2.06	−26.0
	B	22.0	4.27	−23.4
	C	23.2	1.78	−23.4
ρ = 5000, R_{gr} = 165	A	46.1	3.50	−3.91
	B	43.5	3.49	−3.35
	C	46.1	2.41	−3.76

used to consider the effect of the lossy ground on the electric field for the proposed method [69], [70].

Earth return impedance was calculated using formulae shown in [71], [72], and the FD characteristics were considered. A multiphase matching circuit was connected to both ends of each line.

4) Lightning Channel and Source Models: The current distribution along the channel was modeled by the transmission line model with a return stroke speed of 100 m/μs, which is the same representation as the FDTD method. The electric field radiated from the channel was calculated by the potential formulae shown in Section II-A2. In addition, the channel impedance Z_{ch} was set to infinity to achieve the same analysis condition as the FDTD method. The same source model was employed in all EMT analysis models.

For the proposed method, the base height of the lightning channel modeled by the potential method was set slightly higher than the actual base height to achieve higher accuracy. In EMT analysis, the current source was connected to OHGW G_1 for the 500 kV tower and for both 275 kV vertical and horizontal towers, and to the top of the 77 kV tower, following the FDTD analysis. Similarly to the 3D analysis, the lightning strike to each point should be considered in the proposed method, but the base

TABLE V
SAME AS TABLE IV, BUT FOR THE 275 KV DOUBLE-CIRCUIT TOWER

ρ [Ωm], R_{gr} [Ω]	Phase	FDTD [V/A]	Proposed %	Simple %	Multi-story, %
ρ = 0, R_{gr} = 0	U_1	18.3	−0.85	−51.5	−36.5
	M_1	15.9	0.03	−48.5	−39.8
	L_1	12.8	1.51	−45.9	−47.0
ρ = 100, R_{gr} = 2.77	U_1	20.2	−3.74	−51.4	−39.2
	M_1	18.1	−3.91	−48.8	−42.9
	L_1	15.3	−4.05	−46.9	−50.0
ρ = 500, R_{gr} = 13.9	U_1	23.7	−1.37	−41.9	−34.0
	M_1	22.2	−0.89	−37.1	−35.1
	L_1	20.0	−0.32	−32.5	−37.7
ρ = 1000, R_{gr} = 27.7	U_1	26.8	1.80	−32.8	−27.7
	M_1	26.0	2.82	−26.6	−26.6
	L_1	24.3	3.88	−20.6	−26.4
ρ = 5000, R_{gr} = 139	U_1	40.2	13.8	−1.93	−1.23
	M_1	43.1	12.9	3.50	2.78
	L_1	45.2	10.8	6.84	4.95

TABLE VI
SAME AS TABLE IV, BUT FOR THE 77 KV TOWER

ρ [Ωm], R_{gr} [Ω]	Phase	FDTD [V/A]	Proposed %	Simple %	Multi-story, %
ρ = 0, R_{gr} = 0	U_1	21.9	−3.84	−58.6	−46.2
	M_1	20.5	−3.31	−57.0	−51.2
	L_1	18.1	−1.40	−55.4	−57.8
ρ = 100, R_{gr} = 3.47	U_1	25.0	−6.55	−57.0	−47.0
	M_1	23.9	−6.53	−55.4	−51.3
	L_1	21.7	−5.57	−53.9	−56.8
ρ = 500, R_{gr} = 17.4	U_1	31.6	−4.62	−45.5	−39.1
	M_1	31.3	−4.34	−42.8	−41.0
	L_1	29.6	−3.45	−40.1	−43.4
ρ = 1000, R_{gr} = 34.7	U_1	38.0	−2.08	−36.0	−31.9
	M_1	38.4	−1.57	−32.7	−32.2
	L_1	37.1	−0.67	−29.7	−32.9
ρ = 5000, R_{gr} = 174	U_1	65.5	7.14	−8.41	−7.56
	M_1	70.6	6.07	−6.68	−6.56
	L_1	72.4	5.19	−5.25	−5.79

height of the lightning channel z_l for calculating the LEMP was set to be 2 m higher than the actual height h_g. This modeling was adopted to achieve higher accuracy and will be discussed in detail in Section IV-B.

IV. RESULTS AND DISCUSSION

A. Insulator Voltage Waveforms

The proposed method can accurately calculate insulator voltages for not only the struck tower but also the nearby towers and can represent differences in the voltages at the struck side and the other side for towers with double OHGWs by incorporating the LEMP effect, as will be presented below. Fig. 7 shows normalized insulator voltage waveforms for the lightning-struck tower (Tower#3) and nearby towers (Tower#2, #1) calculated for a soil resistivity of 500 Ωm. The phase positions were shown in Fig. 3. Note that the tower grounding resistances for this soil resistivity for the 500, 275, and 77 kV vertical double-circuit transmission towers and the 275 kV horizontal single-circuit transmission tower were 8.15, 13.9, 17.4, and 16.5 Ω, respectively; similar values were derived by the FDTD method.

For all the voltage classes and tower types, the proposed method provides the voltages quite similar to the 3D FDTD-computed voltages, whereas the simple and multistory EMT

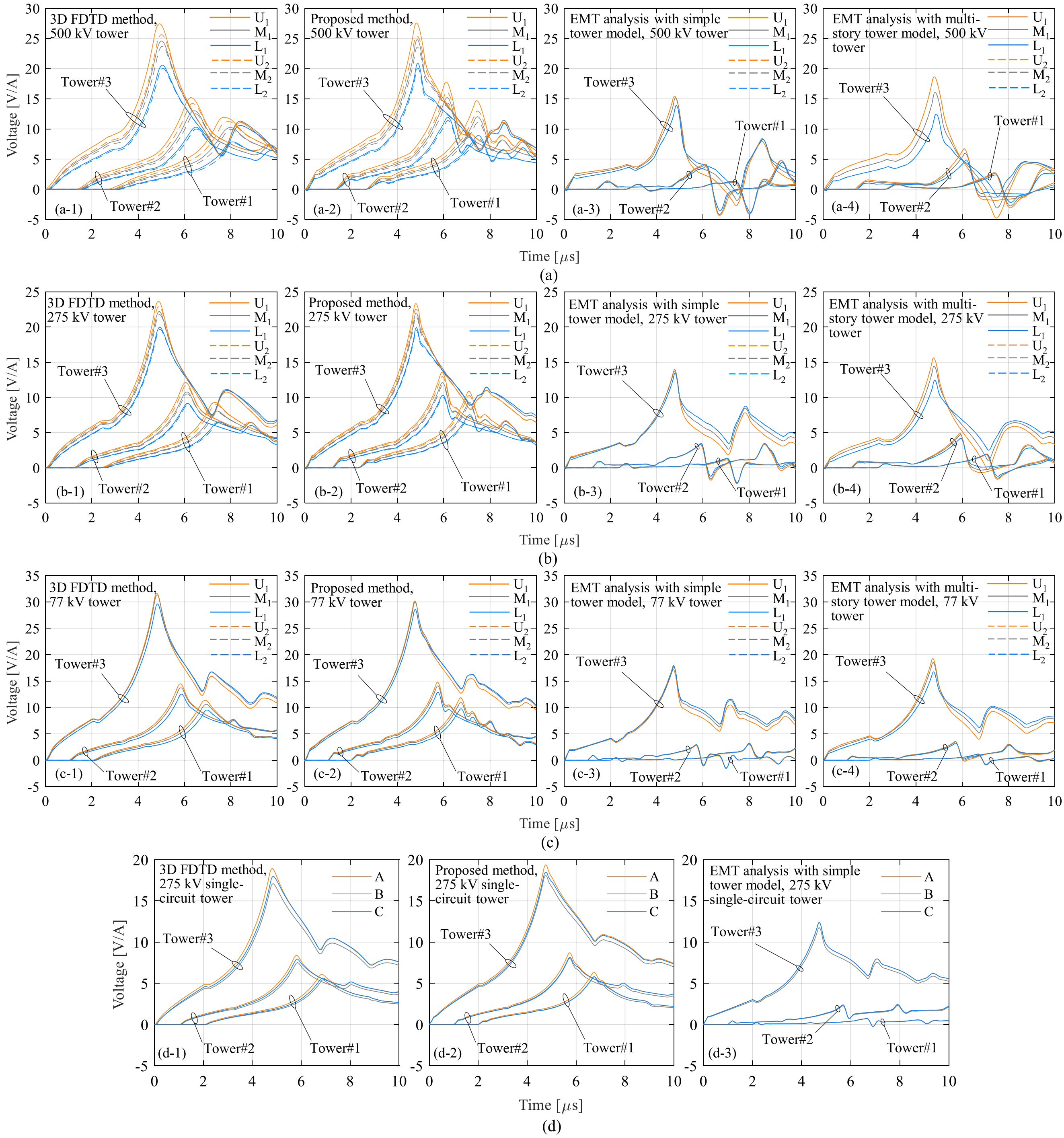

Fig. 7. Normalized insulator voltages calculated by each method for (a) 500 kV, (b) 275 kV, (c) 77 kV double-circuit towers, and (d) 275 kV single-circuit tower for soil resistivity of 500 Ωm. In each row, from left to right, results derived by the following methods are shown: (1) 3D FDTD method, (2) Proposed method (EMT analysis with simple tower model considering the LEMP effect), (3) EMT analysis with simple tower model, and (4) EMT analysis with multistory tower model. Note that the fourth method was not applied to the 275 kV single-circuit tower. For figures in (c), lines showing 1L and 2L (U_1, M_1, L_1, and U_2, M_2, L_2) voltages overlap for all methods since the 77 kV tower has single OHGW and the voltages are generated symmetrically.

analysis models provide lower voltages. This trend is rather significant for the nearby towers than the struck tower. The voltage difference between the struck side (1L) and the other side (2L) can be observed for those computed by the FDTD method and the proposed method (voltages for the 77 kV tower overlapped for 1L and 2L owing to its symmetricity).

Voltage rises contributing to the insulator voltages can be categorized as follows:

1) The voltage rises due to the transient characteristic of the transmission tower.
2) The voltage rises due to the transient characteristic of the overhead lines, namely, the self-surge impedance of the OHGW(s) and the mutual-surge impedance between the OHGW(s) and the phase conductors.
3) The voltage rises due to the transient and steady-state characteristics of the tower grounding.

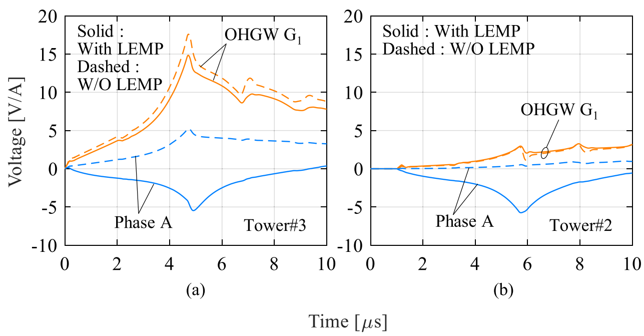

Fig. 8. Normalized voltage rises of the OHGW G_1 and the phase conductor A of the 275 kV single-circuit tower for a soil resistivity of 500 Ωm. (a) voltages at the struck tower (Tower#3) and (b) those at the nearby tower (Tower#2). Solid lines show the results calculated considering the LEMP effect (Proposed), and dashed lines show those calculated without considering the LEMP effect (Simple).

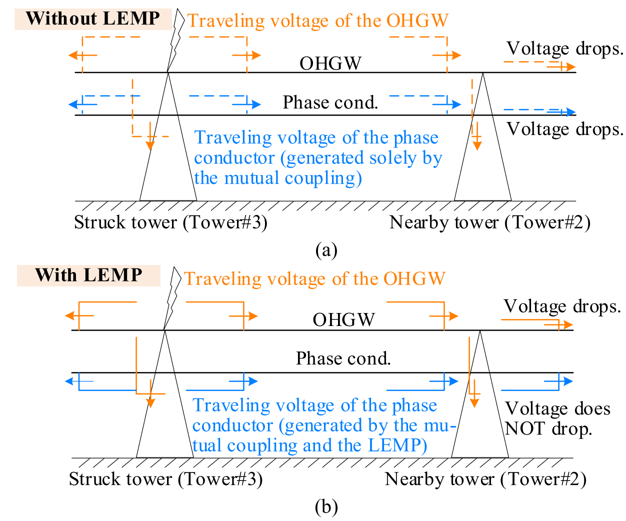

Fig. 9. Conceptual sketch for traveling voltages of OHGW and phase conductor (a) not considering the LEMP effect and (b) considering the LEMP effect.

4) The voltage rises due to the LEMP effect on the OHGW(s) and phase conductors.

The first three voltage rises are generated by the lightning current flowing into the tower, tower grounding, and OHGW(s), whereas the last one is generated by the LEMP effect. The FDTD and proposed methods consider all the contributions, while the conventional EMT analysis does not consider the contribution from the LEMP. Thus, the voltage rises due to the LEMP effect on the OHGW(s) and phase conductors have an important role in determining the insulator voltages.

First, we discuss the reason why the proposed method provides accurate insulator voltages for not only the struck tower but also the nearby towers, whereas the conventional EMT analysis models provide lower voltages. The LEMP effect becomes visible by plotting the voltage rises of OHGW(s) and phase conductors. Fig. 8 shows the normalized voltage rises of OHGW G_1 and the phase conductor A of the 275 kV single-circuit tower for a soil resistivity of 500 Ωm at the struck tower (Tower#3) and nearby tower (Tower#2). The solid lines show the results calculated using the proposed method and the dashed lines show those using the simple EMT analysis model. Since the LEMP generates the voltages having a polarity opposite to those generated by the lightning current, the voltage rises calculated using the proposed method are lower than those calculated using the simple EMT analysis model; the phase conductor voltage even has the opposite polarity. The insulator voltage is given by the difference between the voltages of the OHGW (tower arm) and phase conductor; thus, the higher insulator voltages were derived by the proposed method. The OHGW voltage drops at the nearby tower since the traveling voltage is grounded via the tower. As shown in Figs. 8(b) and 9(a), if the LEMP is not considered, the phase conductor voltage, which is determined by the mutual coupling between the OHGW and the phase conductor, drops according to the OHGW voltage. However, as shown in Figs. 8(b) and 9(b), if the LEMP is considered, the phase conductor voltage does not drop according to the OHGW voltage—the voltage induced by the LEMP travels along the phase conductor without suffering from the voltage drop due to the grounding via the tower. That is why the proposed method provides accurate insulator voltages for both the struck tower and nearby towers, whereas the EMT analysis using simple and multistory models provides lower voltages.

The discussion on the LEMP impact shows the importance to explicitly model the lightning channel and LEMP-induced voltages in numerical simulation. Any better tower model cannot provide accurate insulator voltages, especially for nearby towers, unless the LEMP impact is considered (not including the effect of LEMP can be presumably compensated by the more complex tower modeling for providing accurate voltages at the struck tower, e.g., [24], [25], [33]).

It is worth noting that although the proposed method using the simple tower model can provide accurate insulator voltages, the detailed modeling of the tower is important to improve the accuracy. There are differences between the voltage waveforms calculated by the FDTD method and the proposed method shown in Fig. 7, especially for the vertical double-circuit towers: the voltages calculated by the FDTD method drop a bit slower after their peak and have less oscillations than those calculated by the proposed method. These characteristics are surely related to the traveling wave attenuation along the tower. The improvement of the tower model for the LEMP-considered EMT analysis is one of the important topics to study further.

The differences between the voltages at the struck side and the other side are discussed as follows. For the vertical double-circuit towers with double OHGWs (Fig. 7(a) and (b)), the differences were reproduced by the proposed method owing to the inclusion of the LEMP effect. Since the struck side lines have shorter distances to the lightning channel than the other side lines, the voltages of the phase conductors induced by the LEMP are higher on the struck side. In contrast, for the simple and multistory EMT analysis models, the same voltages are calculated for the struck side and the other side; thus, the symmetrical voltages are derived for both sides. For the 275 kV horizontal single-circuit tower, the voltages at phases A and C become identical for the simple EMT analysis model since the

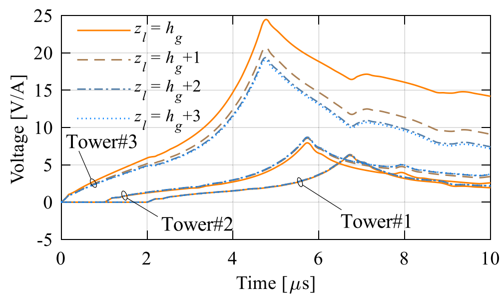

(a)

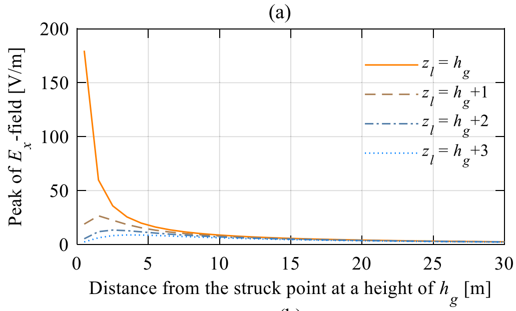

(b)

Fig. 10. (a) Normalized insulator voltages of the phase A and peak values of the normalized incident horizontal electric field to OHGW G_1 (struck side) of the 275 kV horizontal single-circuit tower for soil resistivity of 500 Ωm calculated by the proposed method. Here, the different base height of the lightning channel model z_l was used: z_l was set equal to the height of the OHGW h_g, h_g +1 [m], $h_g + 2$ [m], and $h_g + 3$ [m].

mutual surge impedances between the OHGWs and these phase conductors are identical.

B. Base Height of the Lightning Channel Represented By the Potential Method

As mentioned in Section III-C4, the base height of the lightning channel z_l was set to be 2 m higher than the actual struck height to realize higher accuracy. The reason is shown on the basis of Fig. 10, showing the normalized insulator voltages of phase A and incident horizontal electric field to OHGW G_1 of the 275 kV horizontal single-circuit tower. The figures show the voltages and electric fields calculated by setting the base height z_l equal to OHGW G_1's height h_g and to 1–3 m higher than h_g. When setting the base height z_l equal to h_g, the incident electric field in the vicinity of the struck point becomes very high. Accordingly, the insulator voltage calculated using this model becomes higher (the peak voltage computed by the FDTD method is about 19 V/A, as shown in Fig. 7(d)–(1)). By setting the base height z_l higher than h_g, the electric field in the vicinity of the struck point becomes lower. The insulator voltage converges by setting $z_l = h_g + 2$ [m] and $z_l = h_g + 3$ [m]; hence, the base height $z_l = h_g + 2$ [m] was adopted for the proposed method.

We concur with this modeling from the engineering viewpoint. In the proposed method, the LEMP radiated only from the lightning channel was considered. In an actual phenomenon and in the FDTD method, the LEMP surely radiates from not only the lightning channel but also the OHGWs and the struck tower. Thus, the electric field distribution in the vicinity of the struck point is rather complicated in an actual phenomenon. The proposed method is simply an approximation, and it provides accurate insulator voltages by the base height $z_l = h_g + 2$ [m]. We agree with this representation because (1) the simple tower model can be used in the proposed method, (2) the voltages of nearby towers do not significantly differ depending on the base height, as shown in Fig. 10(a), and (3) accurate insulator voltages can be derived at the struck and nearby towers for various types of towers, as shown in Section IV-A and for a wide range of soil resistivity as shown in the next section.

Note that in [37], in which the basis of the proposed method was presented, a MV distribution line was studied. The length of the pole model for EMT analysis was set to 15 m; accordingly, the height of the channel base was set to 15 m; and the height of the shield wire was 12.25 m: the presented modeling condition was almost satisfied without intension, and accurate insulator voltages were calculated. It was confirmed that the proposed approach can provide accurate overvoltages for different arrangements of MV distribution lines. Thus, the presented modeling can be applied to different types of lines, including transmission and distribution lines.

The presented method neglecting the base few meters of the lightning channel can be considered as the counterpart of the method considering lightning on the ground at some distance from the pole [38], [39], [40], [41]. Comparing the two methods, the proposed method has the following advantages. (1) The proposed method can assume the correct lightning strike location on an *x*-*y* plane; it is probably troublesome to apply the method considering lightning on the ground at some distance from the pole to ultra- and extra-high voltage transmission lines since their crossarms are sometimes longer than 10 m. (2) The proposed method can simulate inclined and tortuous lightning channels by the superposition of the potential formula [48]. Nevertheless, the method considering lightning on the ground at some distance from the pole is novel and powerful method since programs dedicated to indirect lightning events can be applied to direct lightning events.

C. Insulator Voltage Peaks With Various Soil Resistivities

To confirm the accuracy of insulator voltages calculated by the proposed method, Tables IV–VII summarize the insulator voltage peaks of the struck tower calculated by the FDTD method as well as the differences between these voltages and the voltages calculated by the EMT analysis. For the vertical double-circuit towers, the tables show the voltages at the struck side. The differences between the voltages calculated by the FDTD method and the proposed method are less than about 10% for each soil resistivity and each tower. The proposed method can provide accurate insulator voltages for various transmission towers with a wide range of soil resistivities.

The differences between the voltages calculated by the FDTD method and using the simple and multistory EMT analysis models tend to decrease at a higher soil resistivity. This is because the contribution of the voltage rises due to the transient and steady-state characteristic of the tower grounding, mentioned in Section IV-A, becomes more dominant at a higher soil resistivity (high grounding resistance) [25], [73].

In the proposed method, although the differences are still less than about 10%, they are increased at a soil resistivity of

TABLE VIII
CALCULATION TIME FOR EACH LINE BY EACH METHOD FOR THE SOIL RESISTIVITY OF 500 OHMMETER, UNIT IN SECOND

Voltage class [kV]	FDTD	FDTD (HPC)	Proposed method	EMT analysis without LEMP
500	1885	175	42	1.55
275	5042	452	35	1.50
77	11978	956	24	1.28
275-h	14285	1175	19	1.05

5000 Ωm for the 500 and 275 kV vertical double-circuit towers. This result indicates that there is uncertainty in the modeling of the tower grounding characteristic and the tower itself. The tower grounding usually has FD characteristics; in the FDTD method, this frequency dependence is automatically considered, but the constant resistance model was adopted for the proposed method. Moreover, the tower itself can have the FD characteristic owing to the earth-return impedance; this characteristic is considered in the FDTD method, but not in the proposed method. These FD characteristics can have a rather significant impact on the 500 and 275 kV towers owing to their large tower structure and foundations. Although the proposed method provides accurate insulator voltages, these characteristics are worth considered based on the use of relevant EMT analysis models.

D. Summary of Advantages, Limitations, and Possible Modifications of the Proposed Method

First, the calculation time is discussed. Table VIII summarizes the calculation time of the 10 μs transient. A basic computation environment is a 3.0 GHz Intel i7 4-core CPU with 32 GB of RAM and running Windows 10, and OpenMP [74] was used to accelerate the computation for each method. Since the FDTD method is suitable for parallel computations, as an example, the calculation time by a high-performance computer (HPC), NEC's Vector Engine Processor SX-Aurora TSUBASA [75], is shown. Although the proposed method takes a longer calculation time than the EMT analysis not considering the LEMP, the time is much shorter than that of the FDTD method and the calculation is executable in a standard desktop environment.

The advantages of the proposed method can be summarized as follows: (1) accurate insulator voltages can be calculated for not only the struck tower but also the nearby towers; (2) computation by the proposed method is somehow slower than that using the conventional EMT model but much faster than the FDTD analysis: iterative or statistical analysis such as Monte Carlo analysis can be performed with a reasonable calculation time; (3) model parameters can be derived immediately and straightforwardly from the geometries of the tower, tower foundation, and overhead line; (4) the voltage differences between the struck side and the other side can be reproduced; (5) any existing EMT model for representing the tower grounding characteristics (e.g., [76]) can be used; (6) any EMT model for representing the insulator flashover can be used as well (e.g., [12], [31]); (7) inclined, bent, or even a tortuous lightning channel can be modeled.

The limitation is the absence of modeling for reproducing the high-frequency and non-TEM characteristics of the tower and line (e.g., [22], [24]). For the sake of simplicity, in this paper, we adopted the simple tower model considering LEMPs radiated from only the lightning channel. This modeling might be sufficient for judging the occurrence of the back-flashover for various transmission towers since it provides accurate insulator voltages, as shown in Section IV-A and IV-C. However, this modeling cannot represent the high-frequency and non-TEM characteristics of towers and lines. Thus, the accuracy of the model may deteriorate in case of first strokes with very short front duration and subsequent strokes, both including quite high-frequency characteristics. Although the contribution of these strokes on the lightning performance of transmission lines is generally not significant, they are important events to study. A transient phenomenon after the back-flashover occurrence also includes quite high-frequency characteristics.

Modifications for tower and line modeling as well as the consideration of the LEMPs radiated from towers (and lines) may overcome the above-mentioned limitation.

V. CONCLUSION

In this paper, we proposed an EMT analysis method for studying lightning surges at transmission lines considering the LEMP effect. The LEMP effect was incorporated by the potential method for calculating the electric fields and the Agrawal et al. formula for calculating the induced voltages.

According to the analysis using the FDTD analysis results as a reference, the proposed method provides accurate insulator voltages, for not only the struck tower but also the nearby towers, for 500, 275, and 77 kV vertical double-circuit towers and a 275 kV horizontal single-circuit tower for soil resistivities ranging from 0 to 5000 Ωm. In contrast, the EMT analysis without considering the LEMPs provides lower insulator voltages. The LEMPs induce the voltages to both OHGWs and phase conductors, and these voltages have an opposite polarity to the voltages generated by the lightning current flowing into the OHGWs and transmission towers. The high accuracy of the proposed method was achieved since it can consider these LEMP-induced voltages. The difference between the insulator voltages at the struck tower calculated by the FDTD method and the proposed method was less than about 10%.

The models used in the proposed method can be synthesized immediately and straightforwardly from the geometries of the towers and lines, and the transient analysis can be executed with a short calculation time. Thus, the proposed method is a powerful tool for the iterative or statistical analysis of the lightning performance of transmission lines.

REFERENCES

[1] *IEEE Guide for Improving the Lightning Performance of Transmission Lines*, IEEE Standard 1243-1997, 1997 (reaffirmed in 2008).

[2] CIGRE SC33 WG01, "Guide to procedures for estimating the lightning performance of transmission lines," CIGRE, Paris, France, CIGRE Technical Brochure 063, Oct. 1991 (republished in 2021).

[3] CIGRE WG C4.23, "Procedures for estimating the lightning performance of transmission lines-New aspect," CIGRE, Paris, France, CIGRE Technical Brochure 839, Jun. 2021.

[4] Subcommittee for Transmission Lines, Study Committee on Lightning Risk, "Guide to lightning protection design for transmission lines (revised in 2022)," CRIEPI, Yokosuka-shi, Japan, CRIEPI Rep. GD21026, Apr. 2022.

[5] C. A. Jordan, "Lightning computation for transmission line with overhead ground wires," *Gen. Electric Rev.*, vol. 37, no. 3, pp. 180–186, 1934.

[6] M. A. Sargent and M. Darveniza, "Tower surge impedance," *IEEE Trans. Power App. Syst.*, vol. PAS-88, no. 5, pp. 680–687, May 1969.

[7] W. A. Chisholm, Y.I. Chow, and K. D. Srivastava, "Lightning surge response of transmission towers," *IEEE Trans. Power Appar. Syst.*, vol. PAS-102, no. 9, pp. 3232–3242, Sep. 1983.

[8] A. Ametani et al., "Frequency-dependent impedance of vertical conductors and a multiconductor tower model," *IEE Proc. - Gener., Transmiss. Distrib.*, vol. 141, no. 4, pp. 339–345, Jul. 1994.

[9] A. De Conti, S. Visacro, A. Soares, and M. A. O. Schroeder, "Revision, extension, and validation of Jordan's formula to calculate the surge impedance of vertical conductors," *IEEE Trans. Electromagn. Compat.*, vol. 48, no. 3, pp. 530–536, Aug. 2006.

[10] M. Ishii et al., "Multistory transmission tower model for lightning surge analysis," *IEEE Trans. Power Del.*, vol. 6, no. 3, pp. 1327–1335, Jul. 1991.

[11] T. Yamada et al., "Experimental evaluation of a UHV tower model for lightning surge analysis," *IEEE Trans. Power Del.*, vol. 10, no. 1, pp. 393–402, Jan. 1995.

[12] H. Motoyama, K. Shinjo, Y. Matsumoto, and N. Itamoto, "Observation and analysis of multiphase back flashover on the Okushishiku Test Transmission Line caused by winter lightning," *IEEE Trans. Power Del.*, vol. 13, no. 4, pp. 1391–1398, Oct. 1998.

[13] Y. Baba and M. Ishii, "Numerical electromagnetic field analysis on lightning surge response of tower with shield wire," *IEEE Trans. Power Del.*, vol. 15, no. 3, pp. 1010–1015, Jul. 2000.

[14] P. Malicki, S. Papenheim, and M. Kizilcay, "Shielding failure analysis of a hybrid transmission line with AC and DC systems on the same tower," *Electric Power Syst. Res.*, vol. 159, pp. 2–8, Jun. 2018.

[15] E. Stracqualursi, G. Pelliccione, S. Celozzi, and R. Araneo, "Tower models for power systems transients: A review," *Energies*, vol. 15, no. 13, Jul. 2022, Art. no. 4893.

[16] CIGRE WG C4.37, "Electromagnetic computation method for lightning surge studies with emphasis on the FDTD method," CIGRE, Paris, France, CIGRE Technical Brochure 785, Dec. 2019.

[17] K. Yee, "Numerical solution of initial boundary value problems involving Maxwell's equations in isotropic media," *IEEE Trans. Antennas Propag.*, vol. 14, no. 3, pp. 302–307, May 1966.

[18] R. F. Harrington, *Field Computation by Moment Methods*, New York, NY, USA, MacMillan, 1968.

[19] A. E. Ruehli, "Equivalent circuit models for three-dimensional multiconductor systems," *IEEE Trans. Microw. Theory Techn.*, vol. MTT-22, no. 3, pp. 216–221, Mar. 1974.

[20] S. Visacro and A. Soares, "HEM: A model for simulation of lightning-related engineering problems," *IEEE Trans. Power Del.*, vol. 20, no. 2, pp. 1206–1208, Apr. 2005.

[21] B. P. Silva, S. Visacro, and F. H. Silveira, "HEM-TD: New time-domain electromagnetic model for calculating the lightning response of electric systems and their components," *IEEE Trans. Power Del.*, vol. 37, no. 6, pp. 4848–4857, Dec. 2022.

[22] E. Stracqualursi, R. Araneo, J. B. Faria, P. Burghignoli, A. Andreotti, and B. Kordi, "On the transient analysis of towers: A revised theory based on Sommerfeld-Goubau wave," *IEEE Trans. Power Del.*, vol. 38, no. 1, pp. 309–318, Feb. 2023.

[23] J. Takami, T. Tsuboi, K. Yamamoto, S. Okabe, and Y. Baba, "FDTD simulation considering an AC operating voltage for air-insulation substation in terms of lightning protective level," *IEEE Trans. Dielectrics Elect. Insul.*, vol. 22, no. 2, pp. 806–814, Apr. 2015.

[24] A. Yamanaka, N. Nagaoka, and Y. Baba, "Circuit model of vertical double-circuit transmission tower and line for lightning surge analysis considering TEM-mode formation," *IEEE Trans. Power Del.*, vol. 35, no. 5, pp. 2471–2480, Oct. 2020.

[25] M. Saito, M. Ishii, M. Miki, and K. Tsuge, "On the evaluation of the voltage rise on transmission line tower struck by lightning using electromagnetic and circuit-based analyses," *IEEE Trans. Power Del.*, vol. 36, no. 2, pp. 627–638, Apr. 2021.

[26] CIGRE WG C4.39, "Effectiveness of line surge arresters for lightning protection of overhead transmission lines," CIGRE, Paris, France, CIGRE Technical Brochure 855, Dec. 2021.

[27] F. M. Gatta, A. Geri, S. Lauria, M. Maccioni, and A. Santarpia, "An ATP-EMTP Monte Carlo procedure for backflashover rate evaluation: A comparison with the CIGRE method," *Electric Power Syst. Res.*, vol. 113, pp. 134–140, Aug. 2014.gg

[28] Z. G. Datsios, P. N. Mikropoulos, and T. E. Tsovilis, "Closed-form expressions for the estimation of the minimum backflashover current of overhead transmission lines," *IEEE Trans. Power Del.*, vol. 36, no. 2, pp. 522–532, Apr. 2021.

[29] A. Yamanaka, N. Nagaoka, and Y. Baba, "Lightning surge analysis of HV transmission line: Bias AC-voltage effect on multiphase back-flashover," *IEEE Trans. Power Del.*, vol. 36, no. 6, pp. 3570–3579, Dec. 2021.

[30] F. S. Almeida, F. H. Silveira, and S. Visacro, "A new approach for considering the effect of the power-frequency voltage on the calculated lightning performance of transmission lines," *IEEE Trans. Power Del.*, vol. 38, no. 3, pp. 2141–2148, Jun. 2023.

[31] Z. G. Datsios, D. G. Patsalis, P. N. Mikropoulos, and T. E. Tsovilis, "Effects of approximating recorded lightning currents with CIGRE waveforms on computed fast-front overvoltages and critical lightning currents causing flashover to overhead transmission lines," *IEEE Trans. Power Del.*, vol. 38, no. 5, pp. 3084–3094, Oct. 2023.

[32] A. Yamanaka, N. Nagaoka, and Y. Baba, "Circuit model of an overhead transmission line considering the TEM-mode formation delay," *IEEJ Trans. Elect. Electron. Eng.*, vol. 16, no. 6, pp. 888–895, Jun. 2021.

[33] B. Salarieh and B. Kordi, "Full-wave black-box transmission line tower model for the assessment of lightning backflashover," *Electric Power Syst. Res.*, vol. 199, Oct. 2021, Art. no. 107399.

[34] S. Sekioka, T. Nagai, Y. Sonoi, and I. Matsubara, "A computation method of voltages across insulator strings considering the effect of lightning strokes," *IEEJ Trans. Power Energy*, vol. 114, no. 4, pp. 373–380, Apr. 1994.

[35] T. Sonoda, H. Morii, and S. Sekioka, "Observation of lightning overvoltage in a 500 kV switching station," *IEEE Trans. Power Del.*, vol. 32, no. 4, pp. 1828–1834, Aug. 2017.

[36] J. Cao et al., "Lightning surge analysis of transmission line towers with a hybrid FDTD-PEEC method," *IEEE Trans. Power Del.*, vol. 37, no. 2, pp. 1275–1284, Apr. 2022.

[37] A. Yamanaka, K. Ishimoto, and A. Tatematsu, "Direct lightning surge analysis of distribution lines considering LEMPs from lightning channel and struck pole in EMT simulation," *IEEE Trans. Electromagn. Compat.*, vol. 65, no. 6, pp. 1909–1920, Dec. 2023.

[38] F. Tossani et al., "Estimation of the influence of direct strokes on the lightning performance of overhead distribution lines," in *Proc. IEEE Eindhoven PowerTech*, 2015, pp. 1–7.

[39] A. Borghetti, F. Napolitano, C. A. Nucci, and F. Tossani, "Response of distribution networks to direct and indirect lightning: Influence of surge arresters location, flashover occurrence and environmental shielding," *Electric Power Syst. Res.*, vol. 153, pp. 73–81, Dec. 2017.

[40] A. Borghetti, K. Ishimoto, F. Napolitano, C. A. Nucci, and F. Tossani, "Assessment of the effects of the electromagnetic pulse on the response of overhead distribution lines to direct lightning strikes," *IEEE Open Access J. Power Energy*, vol. 8, pp. 522–531, 2021.

[41] K. Ishimoto, F. Tossani, F. Napolitano, A. Borghetti, and C. A. Nucci, "Direct lightning performance of distribution lines with shield wire considering LEMP effect," *IEEE Trans. Power Del.*, vol. 37, no. 1, pp. 76–84, Feb. 2022.

[42] A. K. Agrawal, H. J. Price, and S. H. Gurbaxani, "Transient response of multiconductor transmission lines excited by a nonuniform electromagnetic field," *IEEE Trans. Electromagn. Compat.*, vol. EMC-22, no. 2, pp. 119–129, May 1980.

[43] A. Piantini and J. M. Janiszewski, "Induced voltages on distribution lines due to lightning discharges on nearby metallic structures," *IEEE Trans. Magn.*, vol. 34, no. 5, pp. 2799–2802, Sep. 1998.

[44] F. Rachidi et al., "Current and electromagnetic field associated with lightning-return strokes to tall towers," *IEEE Trans. Electromagn. Compat.*, vol. 43, no. 3, pp. 356–367, Aug. 2001.

[45] J. L. Bermudez et al., "Far-field–current relationship based on the TL model for lightning return strokes to elevated strike objects," *IEEE Trans. Electromagn. Compat.*, vol. 47, no. 1, pp. 146–159, Feb. 2005.

[46] A. Mosaddeghi et al., "Lightning electromagnetic fields at very close distances associated with lightning strikes to the Gaisberg tower," *J. Geophysical Res.: Atmospheres*, vol. 115, 2010, Art. no. D17.

[47] M. Saito, M. Ishii, T. Miki, T. Shindo, and T. Sonehara, "Reproduction of electromagnetic field waveforms of downward lightning strokes hitting Tokyo Skytree," *IEEE Trans. Electromagn. Compat.*, vol. 61, no. 3, pp. 815–822, Jun. 2019.

[48] A. Sakakibara, "Calculation of induced voltages on overhead lines caused by inclined lightning studies," *IEEE Trans. Power Del.*, vol. 4, no. 1, pp. 683–693, Jan. 1989.

[49] A. Tatematsu, "Development of a surge simulation code VSTL REV based on the 3D FDTD method," in *Proc. IEEE Int. Symp. Electromagn. Compat.*, 2015, pp. 1111–1116.

[50] T. Noda, "A numerical simulation of transient electromagnetic fields for obtaining the step response of a transmission tower using the FDTD method," *IEEE Trans. Power Del.*, vol. 23, no. 2, pp. 1262–1263, Apr. 2008.

[51] J. Takami, T. Tsuboi, K. Yamamoto, S. Okabe, Y. Baba, and A. Ametani, "Lightning surge response of a double-circuit transmission tower with incoming lines to a substation through FDTD simulation," *IEEE Trans. Dielectrics Elect. Insul.*, vol. 21, no. 1, pp. 96–104, Feb. 2014.

[52] A. Tatematsu, K. Yamazaki, and H. Matsumoto, "Lightning surge analysis of a microwave relay station using the FDTD method," *IEEE Trans. Electromagn. Compat.*, vol. 57, no. 6, pp. 1616–1626, Dec. 2015.

[53] A. Tatematsu and T. Ueda, "FDTD-based lightning surge simulation of an HV air-insulated substation with back-flashover phenomena," *IEEE Trans. Electromagn. Compat.*, vol. 58, no. 5, pp. 1549–1560, Oct. 2016.

[54] A. Tatematsu, "Lightning surge analysis of a transmission line tower with an XLPE power cable and metallic cleats using the FDTD method," *IEEE Trans. Electromagn. Compat.*, vol. 62, no. 5, pp. 1796–1806, Oct. 2020.

[55] S. Visacro and F. H. Silveira, "Lightning performance of transmission lines: Methodology to design grounding electrodes to ensure an expected outage rate," *IEEE Trans. Power Del.*, vol. 30, no. 1, pp. 237–245, Feb. 2015.

[56] L. Grcev, B. Markovski, and M. Todorovski, "Lightning efficient counterpoise configurations for transmission line grounding," *IEEE Trans. Power Del.*, vol. 38, no. 2, pp. 877–888, Apr. 2023.

[57] Z. P. Liao, H. L. Wong, B. P. Yang, and Y. F. Yuan, "A transmitting boundary for transient wave analysis," *Scientia Sinica*, vol. A27, no. 10, pp. 1063–1076, Oct. 1984.

[58] Y. Baba and V. A. Rakov, "On the transmission line model for lightning return stroke representation," *Geophysical Res. Lett.*, vol. 30, no. 24, p. 17, Dec. 2003.

[59] Y. Baba and V. A. Rakov, "Electromagnetic models of the lightning return stroke," *J. Geophys. Res.*, vol. 112, Feb. 2007, Art. no. D04102.

[60] Z. G. Datsios, P. N. Mikropoulos, and T. E. Tsovilis, "Effects of lightning channel equivalent impedance on lightning performance of overhead transmission lines," *IEEE Trans. Electromagn. Compat.*, vol. 61, no. 3, pp. 623–630, Jun. 2019.

[61] J. Takami and S. Okabe, "Observational results of lightning current on transmission towers," *IEEE Trans. Power Del.*, vol. 22, no. 1, pp. 547–556, Jan. 2007.

[62] T. Noda and S. Yokoyama, "Thin wire representation in finite difference time domain surge simulation," *IEEE Trans. Power Del.*, vol. 19, no. 3, pp. 840–847, Jul. 2002.

[63] E. Stracqualursi, R. Araneo, N. Ravichandran, A. Andreotti, and S. Celozzi, "Modeling of conductors catenary in power lines: Effects on the surge propagation due to direct and indirect lightning," *IEEE Trans. Electromagn. Compat.*, vol. 65, no. 5, pp. 1464–1475, Oct. 2023.

[64] R. Alipio and S. Visacro, "Modeling the frequency dependence of electrical parameters of soil," *IEEE Trans. Electromagn. Compat.*, vol. 56, no. 5, pp. 1163–1171, Oct. 2014.

[65] K. A. Carvalho and F. H. Silveira, "Evaluation of the lightning performance of grounding electrodes using FDTD-based computational model: Influence of absorbing boundary conditions and representation of the frequency-dependence of soil parameters," *Electric Power Syst. Res.*, vol. 213, Dec. 2022, Art. no. 108728.

[66] A. Tatematsu, K. Yamazaki, K. Miyajima, and H. Motoyama, "A study on induced voltages on an aerial wire due to a current flowing through a grounding grid," *IEEJ Trans. Power Energy*, vol. 129, no. 10, pp. 1245–1251, 2009.

[67] K. Yamamoto, S. Yanagawa, K. Yamabuki, S. Sekioka, and S. Yokoyama, "Analytical surveys of transient and frequency-dependent grounding characteristics of a wind turbine generator system on the basis of field tests," *IEEE Trans. Power Del.*, vol. 25, no. 4, pp. 3035–3043, Oct. 2010.

[68] P. L. Bellaschi, R. E. Armington, and A. E. Snowden, "Impulse and 60-cycle characteristics of driven grounds — II," *Elect. Eng.*, vol. 61, no. 6, pp. 349–363, Jun. 1942.

[69] V. Cooray, "Horizontal fields generated by return strokes," *Radio Sci.*, vol. 27, no. 4, pp. 529–537, 1992.

[70] M. Rubinstein, "An approximate formula for the calculation of the horizontal electric field from lightning at close, intermediate, and long range," *IEEE Trans. Electromagn. Compat.*, vol. 38, no. 3, pp. 531–535, Aug. 1996.

[71] E. D. Sunde, *Earth Conduction Effects in Transmission Systems*. New York, NY, USA: Van Nostrand, 1968.

[72] F. Rachidi, C. A. Nucci, and M. Ianoz, "Transient analysis of multiconductor lines above a lossy ground," *IEEE Trans. Power Del.*, vol. 14, no. 1, pp. 294–302, Jan. 1999.

[73] K. Ishimoto, F. Tossani, F. Napolitano, A. Borghetti, and C. A. Nucci, "LEMP and ground conductivity impact on the direct lightning performance of a medium-voltage line," *Electric Power Syst. Res.*, vol. 214, Jan. 2023, Art. no. 108845.

[74] "Home - OpenMP," Accessed: Jul. 31, 2023. [Online]. Available: https://www.openmp.org/

[75] "NEC's Vector Engine processor SX Aurora TSUBASA," Accessed: Jul. 31, 2023. [Online]. Available: https://www.necam.com/VectorEngineProcessor/

[76] R. Alipio, A. De Conti, F. Vasconcellos, F. Moreira, N. Duarte, and J. Martí, "Tower-foot grounding model for EMT programs based on transmission line theory and Marti's model," *Electric Power Syst. Res.*, vol. 223, Oct. 2023, Art. no. 109584.

Akifumi Yamanaka (Member, IEEE) received the B.Sc., M.Sc., and Ph.D. degrees in electrical engineering from Doshisha University, Kyoto, Japan, in 2017, 2019, and 2021, respectively. In 2021, he joined the Central Research Institute of Electric Power Industry, Yokosuka, Japan. His research interests include numerical electromagnetic and EMT analysis of lightning phenomena, and lightning protection of transmission and distribution systems. Dr. Yamanaka was the recipient of the International Conference on Power Systems Transients (IPST) Young Scientist Award in 2023. He is a member of the Institute of Electrical Engineers of Japan, Institute of Electrical Installation Engineers of Japan, and International Council of Large Electric Systems.

Kazuyuki Ishimoto (Member, IEEE) received the B.S., M.S., and Ph.D. degrees in electrical engineering from Waseda University, Tokyo, Japan, in 2007, 2009, and 2018, respectively. Since 2009, he has been with Central Research Institute of Electric Power Industry, Yokosuka, Japan. From 2019 to 2020, he was a visiting Researcher with the Power Systems Laboratory, University of Bologna, Bologna, Italy. His research interests include the area of high voltage, with particular to lightning protection of power systems. He was the recipient of the International Conference on Lightning Protection Young Scientists Awards in 2016. He is currently the Secretary of C4.57 Workings Group of the International Council of Large Electric Systems (CIGRE), Paris, France.

Akiyoshi Tatematsu (Senior Member, IEEE) received the B.E., M.E., and Ph.D. degrees in electrical engineering from Kyoto University, Kyoto, Japan, in 1999, 2001, and 2004, respectively. Since 2004, he has been with Central Research Institute of Electric Power Industry, Yokosuka, Japan. From 2012 to 2013, he was a Postdoctoral Fellow of the Electromagnetic Compatibility Laboratory, Swiss Federal Institute of Technology, Lausanne, Switzerland. He has been engaged in the study of numerical electromagnetic field analysis, electromagnetic transient analysis, and lightning protection of electric power facilities. Dr. Tatematsu is a Distinguished Reviewer of IEEE TRANSACTIONS ON ELECTROMAGNETIC COMPATIBILITY in 2014, 2015, and during 2019–2023. He was the recipient of the International Conference on Lightning Protection Diploma for Young Scientists in 2006 and 2010. He is currently the Chairperson of Japanese National Committee for IEC SC77C and the Secretaries of C4.43 and C4.54 Workings Group of the International Council of Large Electric Systems (CIGRE). He is a member of the IEEJ and CIGRE.